To be presented at the International Conf. on Microelectronic Test Structures (March 1995)

DEPTH MEASUREMENTS USING ALPHA PARTICLES AND UPSETABLE SRAMs

M. G. Buehler, M. Reier, and G. A. Soli
Jet Propulsion Laboratory
California Institute of Technology
Pasadena California 91109

Author - I suggest a global replacement making "over layer" one word.

ABSTRACT

A custom designed SRAM was used to measure the thickness of integrated circuit over layers and the epi-layer thickness using alpha particles and a test SRAM... The over layer consists of oxide, nitride, metal and junction regions.

INTRODUCTION

It is more difficult to measure the thickness integrated circuit layers than the width. Traditional methods such as ellipsometry require areas that are large compared to integrated circuit features, and cross sectioning techniques are time consuming. In this paper, alpha particles are used to measure the over layer and collection layer using a custom SRAM.

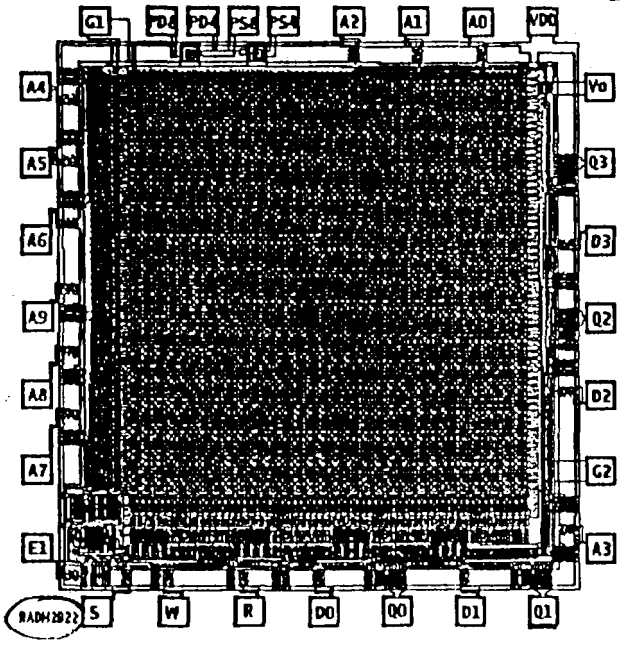

Figure 1. STRV-RADMON chip 2.57 x2.70 mm².

/l'his structure was designed as a radiation monitor, RADMON, and its chip-level layout is shown in Fig. 1. The device is currently flying on the Space Technology Research Vehicle (STRV-1b) in a Geosynchronous Transfer Orbit. This is a joint US-UK project designed to evaluate the effects of space radiation on advanced technology.

The device is a custom designed 4-kbit SRAM with a traditional six-transistor cell [1]. A cross-section through the two inverters which form the memory cell is shown in Fig. 2. As

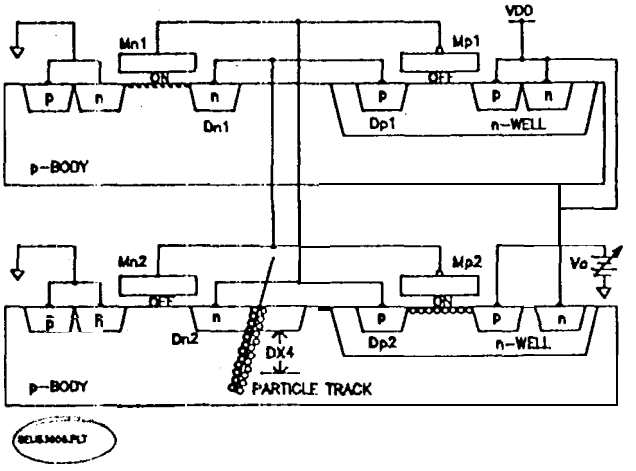

Figure 2. Cross section of the RADMON memory cell showing a particle track creating hole-electron pairs beneath drain Dn2.

indicated in the figure, particles create hole-electron pairs as they pass through the silicon and if enough charge is deposited in the collection layer, DX4, the cell will change state, In the experiments described here, the alpha energy is initially low enough so the alphas do not reach DX4. As the energy is increased the alphas enter DX4 and reach end-of-range before exiting DX4. At higher energies, the alphas pass through DX4 and reach end-of-range in the substrate.

The amount of charge deposited in DX4 will vary according to the Bragg curve. In general, the deposited charge will increase and then decrease as the alpha energy increases.

The cell features an offset voltage, "V_o" connected to inverter #2. This voltage is used to increase the sensitivity of the SRAM to particle upsets by biasing the inverter relative to the cell's metastable point. When biased close to the metastable point, a particle that creates a small amount of charge in DX4 can upset the cell.

In operation the SRAM is written with all ones. Then V_o is lowered and the SRAM is placed in the stare state for a period of time during which the particles flip the cells. Then, V. is raised and the number of zeroes read.

As indicated in Fig. 2, the drain of the n-FET, Mn2, is connected to V. through p-FET Mp2. The drain, Dn2. of Mn2 is enlarged to increase its cross section to articles.

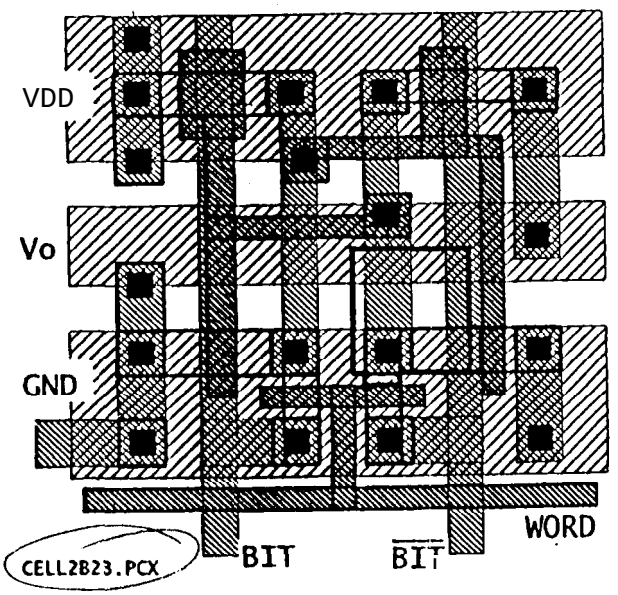

Figure 3. Memory cell layout showing the enlarged drain, Dn2, in bold outline.

This is shown in greater detail in the cell layout shown in Fig. 3 by the area outlined with a bold line. A close inspection of this region indicates that it can be subdivided into three areas each with a different over layer thickness. A cross section of the drain, Dn2, is shown in Fig. 4. There are three distinct areas: (a) no metal (M0), (b) metal-1 or metal-2, (M1&M2) or (c) metal-1 and metal-2 (M1+M2) and these are listed in Table 1. The over layer consist of the insulator layers including the deposited oxides and nitrides, the metal layers, and the diffused junction. The thickness of the three regions and the epi-layer is the subject of this paper.

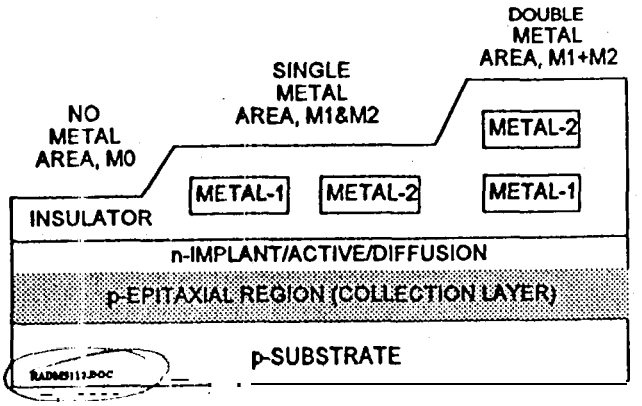

Figure 4. Cross section through sensitive diode Dn2.

Table 1. Over Layer Thickness

REGION	AREA μm²	EST DX3 μm	ALPHA DX3 μm	ALPHA DX4 μm
M0	5.6	4.0	4.3	3.3
METAL-1	7.5	4.8		
METAL-2	12.4	5.4		
M1&M2	19.9	5.3	5.2	3.6
M1+M2	16.6	6.3	6.5	3.6
TOTAL	42,1			

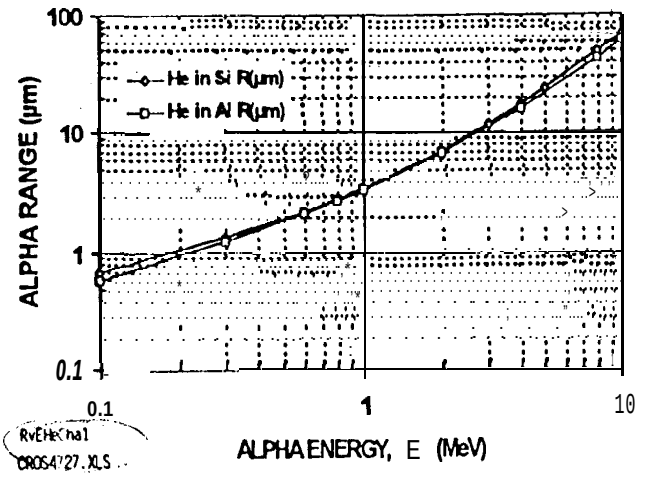

Figure 5. Alpha particle range-energy curve for silicon and aluminum [2].

The range-energy dependence of alphas in silicon and aluminum is shown in Fig. 5. This graph indicates that there is little difference in the range-energy response for alphas in silicon and aluminum. However, for other materials the range-energy relation must be computed as discussed below.

The analysis for the over layer thickness used the energy-range curve for alphas in silicon. An algorithm was fitted to the data shown in Fig. 5. The algorithm is given in the Appendix.

The CMOS over layers consist of a number of different materials and the range of alphas in these materials was converted to an equivalent range in silicon using the Bragg-Kleeman rule [3]:

$$R1/R2 = (\rho 2/\rho 1)\cdot\sqrt{A1/A2} \qquad (1)$$

where ρ is the density and A is the atomic weight of material 1 and 2. In the analysis, material 2 is silicon and the non-silicon layer is material 1. The average thickness of each layer was obtained from the silicon broker, MOSIS. The estimated equivalent silicon thickness for each layer is listed in Table 1.

The nomenclature used to describe the thickness and energy of the layers is shown in Table 2. Experiments were performed in a vacuum of less than 10^{-4} Torr. Gold scattering foils were used to adjust the energy of the alpha particles. The energy of the alpha particles was determined using a pin diode detector and particle spectroscopy equipment. The energy of the alphas as they enter the silicon chip is given by E2.

Table 2. Layer Notation

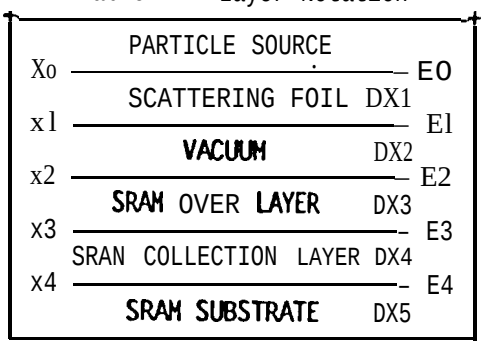

EXPERIMENT

The RADMON was fabricated in a 1.2-μm CMOS process and test results are shown in Fig. 4. These results were derived using the detector equation which describes the rate at which cells are upset:

$$dn/dt = \phi\cdot A_0(N_t - n) \qquad (2)$$

where N_t = 4096 cells, ϕ is the particle flux, A_0 is the memory cell cross section. In the limit where the number of upset cells is small compared with Nt. the cross section is:

$$A_0 = R_0/(\phi\cdot N_t) \qquad (3)$$

where $R_0 = dn/dt|_{t \to 0}$. For this SRAM, A_0 is 42.1 μm^2. The physical meaning of the cross section is the number of upset cells. dn, for a given ϕ, Nt, and dt, the stare time. The stare time is the time the SRAM is exposed to the alpha particles.

In these experiments, the alpha sources were Americium-241 and Gadolinium-148. The incident energy was adjusted using gold scattering foils with various thicknesses. The Am-241 flux was 145 alphas/cm^2·sec with a stare time of 1000 sec. The Gd-148 flux was 87.8 alphas/cm^2· sec with a stare time of 1000 sec.

The results seen in Fig. 6 indicate that the SRAM has a spontaneous (SPON) response when V. is lowered below 1.143 V. The SPON curve has a normally distributed set values due to the spread in cell parameters [1]. This curve is characterized by the mean value, $V_{OS\mu}$. When alpha particles strike the cell, the cells flip at higher V. values which depend on the flux and energy of the particles.

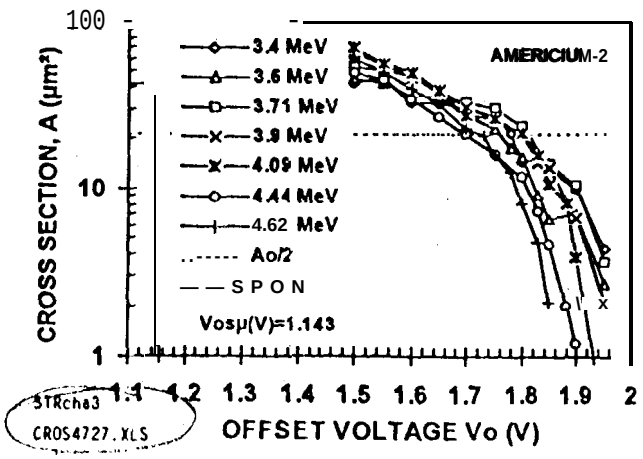

Figure 6 Upset cross section of the SRAM as a function of V. and various alpha particles,

The Am-241 data is shown in greater detail in Fig. 7 and the Gd-148 data is shown in Fig. 8. This data shows that the cross section is significantly greater than A_0 = 42.1 μm^2.

Author - Clarity.

This is due to the capture of charge that strikes regions that active regions such as M0 or M1&M2 or M1+M2.

The results were analyzed at $A_0/2$ and displayed as the square data shown in Fig. 9. At $A_0/2$, half the particle flux has sufficient energy to flip the memory cells due to energy dispersion of the alpha particles. The data Is shown as the differential offset voltage given by the relation: $DV_0 = V_{os\mu}$.

The data plotted in Figs. 7 and 8 shows four distinct regions if plotted as in Fig. 10. A three dimensional representation is shown in Fig. 11. Three distinct peaks are shown on the left-side of the graph and these have been correlated to the three areas of the memory cell.

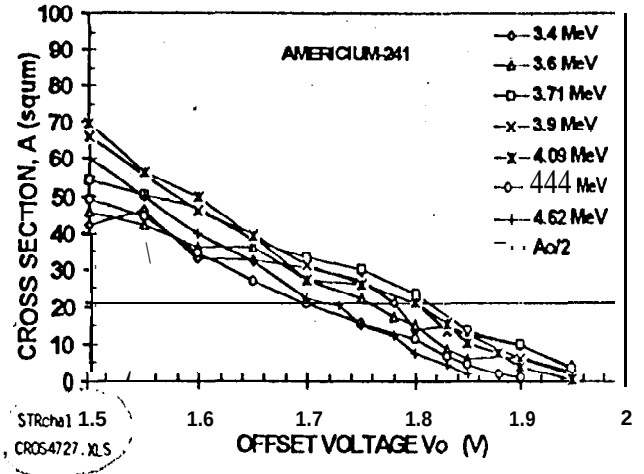

Figure 7. SRAM cross-section versus offset voltage response to Am-241 alpha particles.

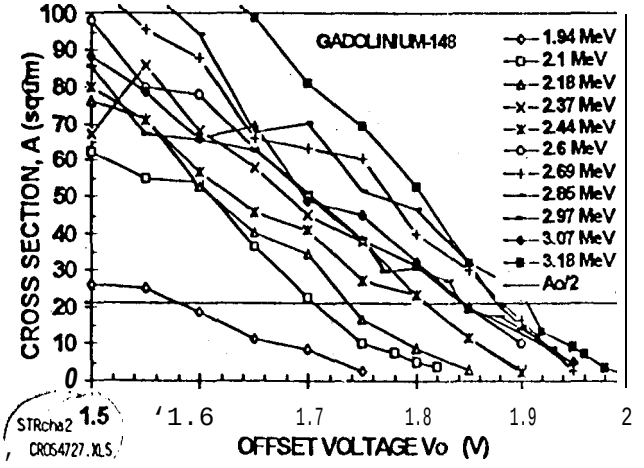

Figure 8. SRAM cross-section versus offset voltage response to Gd-148 alpha particles.

The analysis for the layer thickness is shown by the three solid lines given in Fig. 9.

These curves were obtained assuming values for DX3 and DX4. These parameters were adjusted manually until a reasonable fit was obtained. The energy deposited in the over layer, DX3, is E3 . E4. The range-energy algorithms listed in the Appendix were used in these calculation. The layer thicknesses are listed in the inset of Fig. 9 and in Table 1. The thickness values listed in Table 1 are in good agreement with the thickness estimates derived from the manufacturer's target values.

The solid curves shown in Fig. 9 have three regions. In the first region, particles have insufficient energy to reach DX4 and stop in the DX3. Particles with these low energies will not upset the cells and thus $DV_0 = 0$. Particles with sufficient energy will stop in DX3 and deposit sufficient charge to upset the cells. This is seen as the rising portion of the curves In Fig. 5. Finally, particles with more energy pass through DX4 and stop in DX5. This Is seen as the falling portion of the-curves in Fig. 5. The point at which the alphas just reach DX5 is the point at which the slope of the rising portion of the curve begins to decrease near the top of the curve.

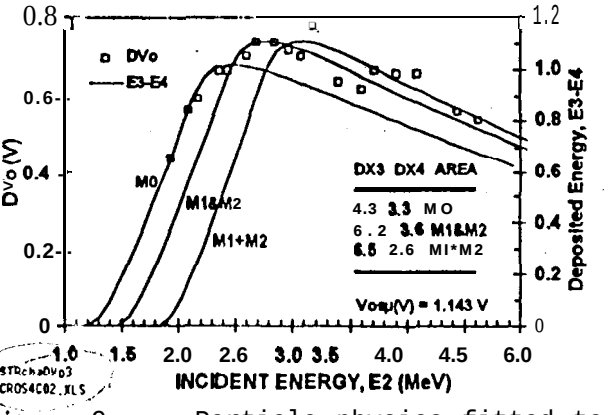

Figure 9. Particle physics fitted to experimental data showing fitted values for the over layer thickness, DX3, and the collection depth, DX4.

An additional layer, which was measured by this technique, is the epi-layer noted as DX4. Two values, 3.3 and 3.6 μm, are listed forDX4 in the inset to Fig. 9.

DISCUSSION

The use of a custom SRAM is shown to have the potential for measuring the over layer and epi-thickness of integrated circuit layers. This method Is effective in measuring the thickness of both conducting and insulating layers. The method require a knowledge of the alpha particle range-energy dependence

and the conversion of the thickness of non-silicon layers to an equivalent silicon thickness.

The memory cell used in this study has regions, with different over layer thicknesses and suffers from the collection of peri heral charge. A simpler structure should be designed with a single over 1 ayer thickness on each memory cell and the cells should be designed with a channel stop to prevent the collection of peripheral charge. The memory could be designed as a scribe-line monitor and used for end-of-line over layer and epi-thickness measurements.

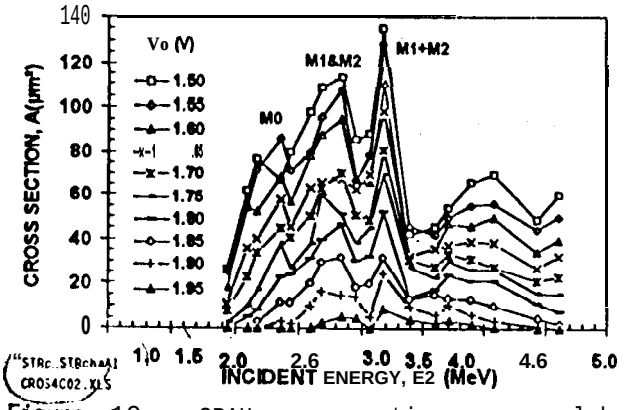

Figure. 10. SRAH cross-section versus alpha energy and V. values showing three major peaks and one minor peak.

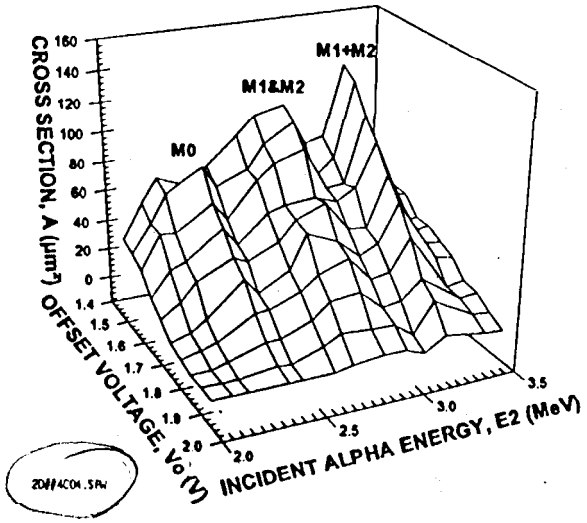

Figure 11. SRAM cross-section response due to three memory cell regions: no metal (MO), Metal-1 and metal-2 (M1&M2), and metal-1 plus metal-2 (M1+M2).

APPENDIX

The range-energy curves [2] for alpha particles in silicon shown in Fig. 4 was fitted with the following parabolic equation where E has units of HeV:

$$Y = \log_{10}(E) = a \cdot X^2 + b \cdot X + c \qquad (A1)$$

where $X = \log_{10}(R)$ and R has units of pm. The coefficients of this equation are:

$$a = -0.2867$$
$$b = 1.4395$$
$$c = -0.7151.$$

The inverse equation was determined by solving the above quadratic equation.

$$X = \log_{10}(R) = A(-1 + \sqrt{[1 - B \cdot (C - Y)]}) \qquad (A2)$$

where

$$A = b/2a = -2.51046$$
$$B = 4a/b^2 = -0.55343$$
$$C = c.$$

It is essential that the inverse equation be derived from the initial a, b, c fitting parameters using this procedure. Attempting to fit the inverse relation, that is the logR vs logE curve, leads to different parameters that ruin the analysis.

REFERENCES

1. H. G. Buehler, B. R. Blaes, and G. A. Soli, "Test SRAMs for Characterizing Alpha Particle Tracks in CMOS/Bulk Memories," International Conference on Microelectronic Test Structures, Vol 4., 113-118 (1991).

2. J. F. Ziegler. *Handbook of Stopping Cross-Sections for Energetic Ions in All Elements*, Pergamon Press (New York, 1980).

3. N. Tsoulfanidis, *Measurement and Detection of Radiation.* Hemisphere Publ. Corp. (New York, 1983) p. 126. . . .

ACKNOWLEDGMENTS

The research described in this paper was performed by the Center for Space Microelectronics Technology, Jet Propulsion Laboratory, California Institute of Technology, and was sponsored by the Ballistic Missile and Defense Organization, Innovative Science and Technology Office. The devices used in this study were fabricated through MOSIS, Information Sciences Institute, University of Southern California, Special thanks go to Vance Tyree, MOSIS, who helped determine the target over layer thicknesses. File: IGMT5324.DOC